Available online at www.sciencedirect.com

ScienceDirect

Procedia Engineering 126 (2015) 290 – 294

Procedia Engineering

www.elsevier.com/locate/procedia

7th International Conference on Fluid Mechanics, ICFM7

Analyses of wave forces on surface piercing vertical cylinders of intermediate scale

Ling Chen, Jifu Zhou*

Key Laboratory for Mechanics in Fluid Solid Coupling Systems, Institute of Mechanics, Chinese Academy of Sciences, Beijing,China

Abstract

Maximum horizontal forces by regular waves on a surface piercing vertical cylinder of intermediate scales are computed by solving the two-phase incompressible Navier-Stokes equations with a VOF method. The incident waves are generated by the fifth order Stokes wave and cnoidal wave. The numerical flume is verified and validated by comparison to the second order Stokes theory and by grid-independence. A variety of scales and wave steepness are computed in deep water and finite depth. In fully nonlinear wave condition, the viscosity and diffraction effects are discussed. A more accurate demarcation of intermediate scales is given by scales (the ratio of the diameter to the wavelength) from 0.1 to 0.125.

Peer-review under responsibility of The Chinese Society of Theoretical and Applied Mechanics (CSTAM)

*Keywords:*wave force, intemediate scale, fully nonlinear, Navier-Stokes/VOF;

1. Introduction

In ocean engineering, cylindrical structures of different scales have been widely used. The scales tend to become larger and larger, such as monopiles, platform caps and gravity base supports. Conventionally, the structures are treated as small or large scale according to their relative horizontal dimensions to wavelength. Therefore, the horizontal wave load can be estimated by Morison equation for small scale piles [1], and by diffraction theory for large scale ones [2], respectively. However, due to the changes of structure dimensions and wave climate as well, there are certainly some cases in which the structures are neither of small scale nor of large scale. Moreover, the

* Corresponding author. Tel.: +86-010-82544203
E-mail address: zhoujf@imech.ac.cn

Peer-review under responsibility of The Chinese Society of Theoretical and Applied Mechanics (CSTAM)
doi:10.1016/j.proeng.2015.11.245

demarcation of small and large scales seems to be variable in previous literatures and lack of strong dependence in engineering applications. In addition, the traditional knowledge is mainly based on linear or weak nonlinear theories. Therefore, it is of great significance to explore the estimation approach of wave loads for the structures of intermediate scale, especially for nonlinear wave cases.

Fully nonlinear numerical investigations of wave forces on monopoles have been undertaken by many authors, with a main focus on the small scale cylinders and its higher-harmonic wave forces. Christensen et al [3] computed the regular wave forces of a monopile on a sloping sea bed. Paulsen et al [4] presented the fully wave forcing on a bottom-mounted circular cylinder in waters of intermediate depth and discussed the second load. But few studies of wave force on cylinders of intermediate scale are available. In the present paper we extend the research on fully nonlinear wave forcing on surface piercing vertical cylinders of intermediate scale.

2. Numerical methods

Linear and weak nonlinear models for free-surface and force analysis are based on the Morison equation and diffraction theory. For fully nonlinear wave conditions, Navier-Stokes equations are generally used to describe the free surface which is large deformation and even breaking especially around the structures. The incompressible Navier-Stokes solver, named interFoam, which is a part of the open source CFD toolbox OpenFOAM, is used here. It is designed for simulating the evolution of the interface between two phases at constant temperature. The interface is captured through the VOF technique [5] and a combined algorithm PISO-SIMPLE is adopted to solve the velocity-pressure coupling. This solver was further extended into the waves2Foam by Jacobsen et al with a fully nonlinear wave generation and absorption program, through which we can easily simulate the target wave environment [6].

First, it is necessary to establish a numerical wave flume. Waves are generated by giving free surface elevation and velocity profile at the left vertical wall every time step. They also are corrected by the target wave in a follow relaxation zone [6]. At the downstream end of the flume, a similar zone is used to absorb wave energy. This method of wave generation is in agreement with the target wave and efficiently prevents secondary reflections caused by the influence of structures. In this way, the numerical domain is smaller and thus reduces the computation time, because the structure can be sited quite close to the wall of wave generation.

To verify the numerical flume, an example of second order Stokes wave is presented. The wave flume has a length of 10m and a height of 0.65m, with the other parameters of depth h=0.5m, wave height H=0.12m, wave period T=1.5s and wave length L=2.82m. Both the wave generation and absorb zone are 2.8m long in the upstream and downstream of the flume respectively. A wave gauge is located at x=3m.Time history of wave surface elevation compared with the 2nd-order Stokes theory is shown in Fig.1. An excellent agreement is observed apparently.

In the direction of propagation, the wave height would be decay if the numerical grids are sparse. Grid-independency of the results is assessed by the discretizations of 5, 10 and 15 points per wave height (PPWH) and 40, 50, 60 and 70 points per wave length (PPWL). Parameters are the same as the above case except that the wave flume length is extended to 30m instead of 10m.The errors between the theoretical and computed results as a function of time normalized by the wave period are presented in Fig.2. We can easily find that the errors increase with propagation distance, and a good grid-independence can be achieved if PPWH>10 and PPWL>60.

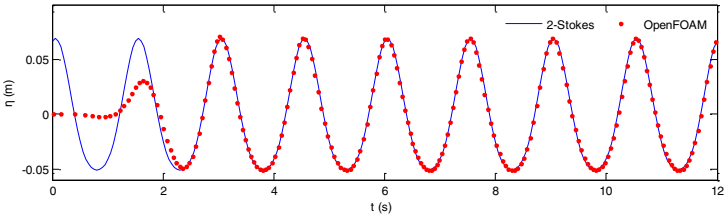

Fig. 1. Comparison between theory and numerical reproduction of free surface elevation using OpenFOAM

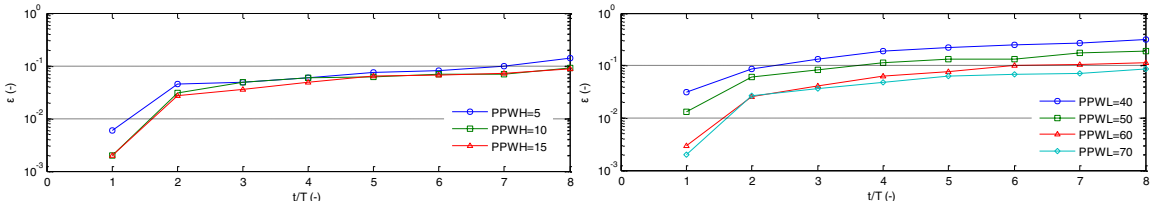

Fig. 2. Errors between the theory and numerical results of different grids as a function of time.

3. Results

3.1. Dimensional analysis

In cases of simple regular waves on flat bed, the maximum horizontal wave force F on a bottom-mounted cylinder during a wave period can be considered as a function of the following dimensional parameters: wave height H, depth h, wave length L, diameter D, density ρ, gravity g, and kinematic viscosity ν. Taking ρ, g, L as the three basic parameters, we have

$$\frac{F}{\rho g A D^2} = f\left(\frac{H}{L}, \frac{h}{L}, \frac{D}{L}, \frac{\nu}{\sqrt{gL^3}}\right) = f\left(kA, \mathrm{kh}, kR, \mathrm{Re}\right) \tag{1}$$

Where k is the wave number, A is half of wave height in deep water, R is cylinder's radius, Re is Reynolds number. In shallow or finite depth water, the effect of depth on wave height is greater than the wavelength's. Therefore, the function can be written as:

$$\frac{F}{\rho g A D^2} = f\left(\frac{H}{H_{\max}}, \mathrm{kh}, kR, \mathrm{Re}\right) \tag{2}$$

where $H_{\max}$ is the critical breaking wave height.

3.2. Studied cases and wave generation

11 cases of deep water (indicated by ▲ and ●) and 3 cases of finite depth (indicated by ○) are designed for case studies. The dimensionless parameter D/L for surface piercing vertical cylinder of intermediate scale varies from 0.1 to 0.2. Considering the similar theorems and easy operation, the depth in the test cases of deep water are chosen as 12m. A graph of studied non-dimensional parameter space is shown in Fig.3, and the complete parameters of all cases are list in table 1. The wave generations are based on fifth order Stokes waves for the deep water, while other three cases are cnoidal waves for finite depth according to Méhauté [7]. The values of H are measured at the location by the transverse side of the cylinder but far away from it. Hence, the wave height would be measured accurately with little influence of cylinder. By the way, in order to reduce the computation time, a symmetrical plane boundary condition is used. We also had verified the wave forces on vertical cylinder in weak nonlinear wave condition as well as wave generation.

Table 1. Parameters for the incident waves.

h (m)	H (m)	T (s)	L (m)	D (m)	kh (-)	kR (D/L) (-)	kA (-)	KC (-)	H/H_{max} (-)	
12	0.99	4.00	24.87	2.50	3.03	0.316 (0.10)	0.125	1.056	—	▲

12	1.40	4.00	24.87	2.50	3.03	0.316 (0.10)	0.177	1.552	—	▲
12	1.82	4.00	24.87	2.50	3.03	0.316 (0.10)	0.230	1.968	—	▲
12	0.99	4.00	24.87	3.75	3.03	0.474 (0.15)	0.124	0.736	—	▲
12	1.48	4.00	24.87	3.75	3.03	0.474 (0.15)	0.187	1.163	—	▲
12	1.97	4.00	24.87	3.75	3.03	0.474 (0.15)	0.249	1.461	—	●
12	0.99	4.00	24.87	5.00	3.03	0.632 (0.20)	0.125	0.568	—	▲
12	1.44	4.00	24.87	5.00	3.03	0.632 (0.20)	0.182	0.864	—	▲
12	1.89	4.00	24.87	5.00	3.03	0.632 (0.20)	0.239	1.120	—	▲
12	1.85	4.00	24.87	3.125	3.03	0.395 (0.125)	0.233	1.702	—	▲
12	1.82	4.00	24.87	4.375	3.03	0.553 (0.175)	0.229	1.271	—	▲
12	3.79	8.16	75.00	11.25	1.01	0.471 (0.15)	0.159	1.559	0.836	○
10	3.44	8.34	75.00	11.25	0.84	0.471 (0.15)	0.144	1.631	0.860	○
8	2.93	8.77	75.00	11.25	0.67	0.471 (0.15)	0.123	1.692	0.870	○

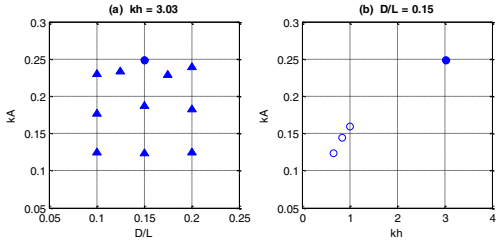

Fig. 3. A graph of studied non-dimensional parameter space.

3.3. Wave forces

Maximum horizontal wave forces predicted by linear models are compared with the corresponding numerical results. All results are normalized by $\rho g A D^2$ and shown explicitly in Fig.4 as a function of incident wave steepness kA which varies from 0.12 to 0.25. Fig.4 (a)~(c) are respectively for three different cylinders of intermediate scale. It may be noted that the results of diffraction are independent of kA, while Morison equation's results slightly increase with kA. These tendencies are probably relevant to the drag force relating to viscous effect. From Fig.4 (a) of relatively small scale cylinder, the numerical results are almost equal to the theory especially for small wave height. But inform Fig.4 (b) and (c) for relatively larger scales, the linear models overestimate the horizontal wave force. In Fig.4 (b), the maximum errors for linear diffraction theory and Morison equation relative to numerical results are 6.7% and 9.4% respectively, while in Fig.4 (c), they are 9.6% and 20.2%. Fig.4 (d) shows the maximum force of various scales for large kA. These phenomena may be due to the cylinder induced turbulence in wave field, which leads to the smaller inertial force relating to diffraction effect. On the one hand, the turbulence also grows with wave height, so that the normalized maximum force turns to decrease, which can be confirmed by linear diffraction theory. On the other hand, the increasing wave height also increases the turbulence, the decreasing trend of the normalized maximum force can be found in these fully nonlinear numerical computations. For Fig.4 (a), the viscous effect cannot be neglected for large kA. Hence, the total forces including viscous and diffraction effects slightly increase with kA. For small kA, both viscous and diffraction effects are too small to play a role in wave force for cylinder of intermediate scales. A good agreement of results between Morison equation and diffraction theory in the scales ranged from 0.05 to 0.2 can be found. For large kA, both the viscous and diffraction effects cannot be neglected. They are more important respectively for smaller and larger cylinders. It is interesting to find that the viscous effect increases the maximum horizontal forces while diffraction effect decreases it. As a result, it might be found a balance point between scales of 0.1 and 0.125 according to Fig.4 (d). That means the demarcation of small and large scales may be defined in this range.

In finite depth water, the maximum horizontal wave forces are underestimated seriously by linear models (Fig.5). Depth is the parameter that influences the wave forces greatly. In case of small water depth, the nonlinearity of waves is much stronger than that in deep water. The viscous effect becomes more significant. In the studied cases of 8m depth, diffraction theory and Morison equation underestimate the wave force by 18.5% and 17.5% respectively.

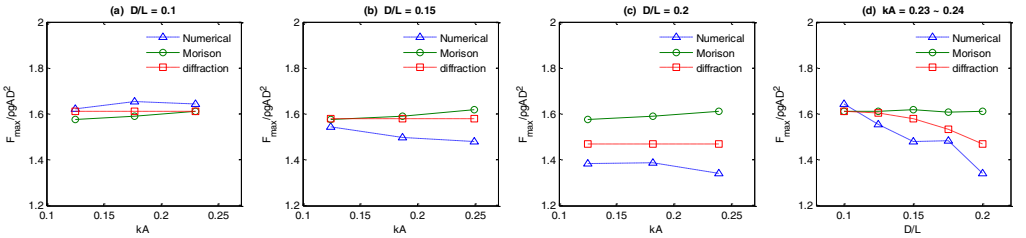

Fig. 4. Maximum horizontal wave force in deep water.
(a) D/L=0.1 kh=3.03; (b) D/L=0.15 kh=3.03; (c) D/L=0.2 kh=3.03; (d) D/L=0.15 kA=0.23~0.24

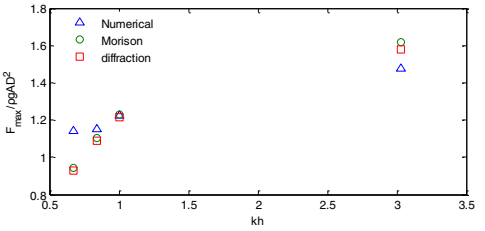

Fig. 5. Maximum horizontal wave force in finite depth water and compared with that in deep water.

4. Conclusion

A numerical flume has been established, which is grid-independent and verified by second order Stokes theory with an excellent agreement. The flume is applied to investigate maximum horizontal wave forces on a surface piercing vertical cylinder of intermediate scale in the cases of deep and finite depth water.

In deep water, with the increasing of wave steepness, the viscous effect increases faster than diffraction effect for the scale of 0.1, increasing the total horizontal force. And the diffraction effect apparently increases for the scales of 0.15 and 0.2, decreasing the total horizontal forces. The demarcation of small and large scale cylinders may be defined between 0.1 and 0.125 according to the present numerical results. In finite depth water, the nonlinearity of waves is stronger than in deep water. The viscous effect gets apparent rapidly with depth decreasing.

References

[1] J.R. Morison, M.P. O'Brien, J.W. Johnson, S.A. Schaaf, The forces exerted by surface waves on piles, J. Petrol. Tech. 1950, 2 (5), 149-154.
[2] R.C. MacCamy, R.A. Fuchs, Wave forces on piles: a diffraction theory, Tech.Mem. 69, US Army Coastal Engineering Research Center, 1954.
[3] E.D. Christensen, H. Bredmose, E.A. Hansen, Extreme wave forces and run-up on offshore wind turbine foundations, In Proc. Copenhagen Offshore Wind, 2005.
[4] Bo.T. Paulsen, H. Bredmose, H.B. Bingham, N.G. Jacobsen, Forcing of a bottom-mounted circular cylinder by steep regular water waves at finite depth, J. Fluid Mech. 2014, vol. 775, pp. 1-34.
[5]C.W. Hirt, B.D. Nichols, Volume of fluid (VOF) method for the dynamics of free boundaries, J. Comput. Phys. 1981, 39, 201-225.
[6] N.G. Jacobsen, D.R.Fuhrman, J.Fredsø, A wave generation toolbox for the open-source CFD library: openfoam®. Intl J. Numer. Meth. Fluids, 2012, 70 (9), 1073-1088.
[7] B.L. Méhauté, An introduction to hydrodynamics and water waves, SpringerVerlag, New York, 1976.